Title

Characterization of heart macrophages in rhesus macaques as a model to study cardiovascular disease in humans

Journal

Journal of Leukocyte Biology, 106(6)

ISSN

0741-5400

Authors

Petkov, Daniel I
Liu, David X
Allers, Carolina
et al.

Publication Date

2019-11-28

DOI

10.1002/jlb.1a0119-017r

Peer reviewed

HHS Public Access

Author manuscript

J Leukoc Biol. Author manuscript; available in PMC 2020 May 12.

Published in final edited form as:

J Leukoc Biol. 2019 December ; 106(6): 1241–1255. doi:10.1002/JLB.1A0119-017R.

Characterization of heart macrophages in rhesus macaques as a model to study cardiovascular disease in humans

Daniel I. Petkov[1,4], **David X. Liu**[2,5], **Carolina Allers**[1], **Peter J. Didier**[2], **Elizabeth S. Didier**[3,*], **Marcelo J. Kuroda**[1,*]

[1]Division of Immunology, Tulane National Primate Research Center, Covington, Louisiana, USA

[2]Division of Comparative Pathology, Tulane National Primate Research Center, Covington, Louisiana, USA

[3]Division of Microbiology, Tulane National Primate Research Center, Covington, Louisiana, USA

[4]Charles River Laboratories Edinburgh, Ltd., Tranent, United Kingdom

[5]Integrated Research Facility, Division of Clinical Research, National Institute of Allergy and Infectious Diseases (NIAID), Bethesda, Maryland, USA

Abstract

Rhesus macaques are physiologically similar to humans and, thus, have served as useful animal models of human diseases including cardiovascular disease. The purpose of this study was to characterize the distribution, composition, and phenotype of macrophages in heart tissues of very young (fetus: 0.5 years, $n = 6$), young adult (2–12 years, $n = 12$), and older adult (13–24 years, $n = 9$) rhesus macaques using histopathology and immunofluorescence microscopy. Results demonstrated that macrophages were uniformly distributed throughout the heart in animals of all age groups and were more prevalent than CD3-positve T-cells and CD20-positive B-cells. Macrophages comprised approximately 2% of heart tissue cells in the younger animals and increased to a mean of nearly 4% in the older adults. CD163-positive macrophages predominated over HAM56-positive and CD206-positive macrophages, and were detected at significantly higher percentage in the animals between 13 and 24 years of age, as well as in heart tissues exhibiting severe histopathology or inflammation in animals of all age groups. In vivo dextran labeling and retention indicated that approximately half of the macrophages were longer lived in healthy adult heart tissues and may comprise the tissue-resident population of macrophages. These results provide a basis for continued studies to examine the specific functional roles of macrophage

Correspondence: Marcelo J. Kuroda, Center for Comparative Medicine and California National Primate Research Center, University of California at Davis, County Road 98 and Hutchison Drive, Davis, CA 95616, USA. mjkuroda@ucdavis.edu.

*Current address: Center for Comparative Medicine, Unit of Infectious Diseases, California National Primate Research Center University of California—Davis, County Road 98 and Hutchison Drive, Davis, CA 95616, USA.

AUTHORSHIP

D.I.P., D.X.L., and P.J.D. performed the experiments and histopathology. D.I.P., D.X.L., C.A., P.J.D., E.S.D., and M.J.K. contributed to the experimental design, data analyses, interpretation of results for preparation of figures and tables, and writing the manuscript.

DISCLOSURES

The authors report no financial conflicts of interest.

SUPPORTING INFORMATION

Additional information may be found online in the Supporting Information section at the end of the article.

subpopulations in heart tissues during homeostasis and in cardiovascular disease for then developing intervention strategies.

Graphical Abstract

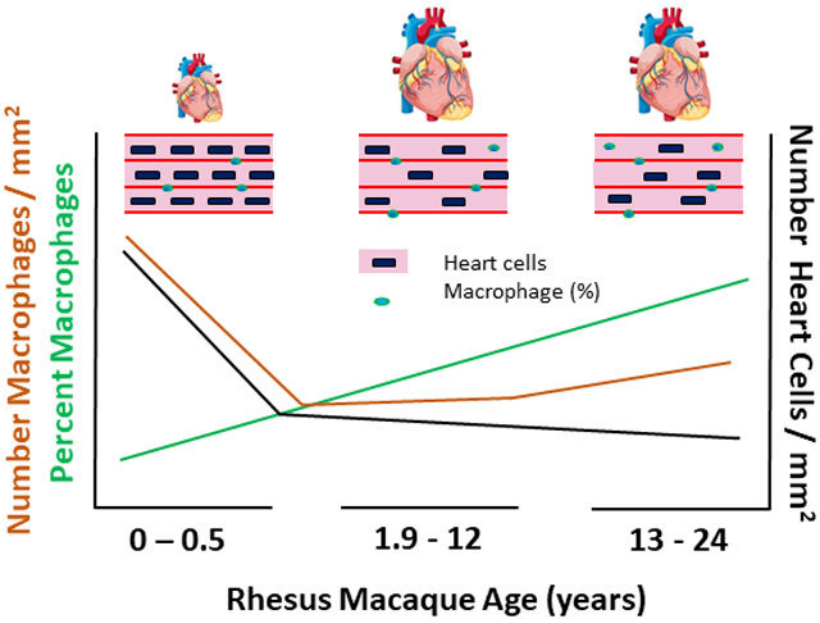

Keywords

cardiac muscle; immunofluorescence; microscopy; skeletal muscle

1 INTRODUCTION

Myocarditis is often reported in cases of sudden cardiac death or unexplained cardiomyopathy in humans and rhesus macaques (*Macaca mulatta*).[1–3] An accurate characterization of the different levels of severity in myocarditis in relation to disease outcome, however, is still challenging.[4–6] Cells of the mononuclear phagocyte system, specifically monocytes and macrophages, participate in tissue regeneration, innate inflammatory and adaptive immune responses, and tissue repair to help re-establish homeostasis.[7–10] Heterogeneous populations of macrophages exist in different organs, such as lung[11–13] and heart[14–18] of mammals, including humans, rhesus macaques, and mice[19–21] that are necessary for regulating immune responses, as well as tissue repair. Macrophage population imbalances and cell dysfunction, however, may adversely impact the host through tissue damage including reduced cardiac function.[22]

Recent work in mice demonstrated that tissue-resident macrophages originate from progenitor cells within the yolk sac that developed during embryogenesis and “transitory myeloid cells” from hematopoietic stem cells within bone marrow.[14,23–25] The self-renewal capacity of embryo-derived cardiac macrophages in normal heart declines with age and these macrophages are slowly replaced by monocytes from blood.[17] Phenotypic

characteristics of cardiac macrophages at varying ages and health conditions are difficult to study in humans because most samples are obtained postmortem, and there are limited numbers of antemortem biopsies available for research. One such recent report examining left ventricular myocardial specimens from human patients with dilated and ischemic cardiomyopathies demonstrated the presence of discernible macrophage subpopulations based on CCR2 expression.[18] From gene expression profiles, the authors suggested that the CCR2-negative population was from tissue resident self-renewing macrophages, while the CCR2-positive population resembled monocyte-derived tissue macrophages.[15,18,26]

Little information exists about macrophage characteristics in normal or relatively healthy human heart tissue. Rhesus macaques provide a useful model to study the roles and characteristics of macrophages in both normal and diseased heart tissue due to their similar physiology to humans.[27,28] Thus, studies using rhesus macaques are expected to translate to humans for developing intervention strategies to improve heart disease conditions. In previous studies from our laboratory on lung tissues in healthy rhesus macaques, we identified unique macrophage populations on the basis of CD163 and CD206 expression among other features,[11] and subsequently demonstrated that increased monocyte turnover in blood reflected a direct relationship to macrophage tissue destruction during SIV infection and progression to terminal AIDS.[29,30] The purpose of this current report was to characterize macrophages in heart tissues of rhesus macaques with and without disease. In addition to examining macrophage distribution and surface phenotype, we applied in vivo dextran inoculation to identify longer-lived, presumably resident, heart tissue macrophages. The results further support the presence of distinct macrophage populations in heart and help establish a rhesus macaque model to study the roles of macrophages in cardiovascular diseases that can then be translated to developing treatment strategies in humans.

2 MATERIALS AND METHODS

2.1 Animals and dextran administration

Rhesus macaques (*M. mulatta*) of Indian origin used in this study were housed at the Tulane National Primate Research Center, had not been experimentally inoculated with infectious agents, and were SPF for *Macacine herpesvirus* 1, simian immunodeficiency virus, simian retrovirus, and simian T-lymphotropic virus 1, as well as negative for measles virus and *Mycobacterium tuberculosis*. All procedures were performed in accordance with the National Institutes of Health *Guide for the Care and Use of Laboratory Animals*[31] and the Association of the Assessment and Accreditation of Laboratory Animal Care, and were approved by the Institutional Animal Care and Use Committee of Tulane University.

Heart and skeletal muscle tissues were examined from a total of 27 rhesus macaques ranging from fetal through 24 years of age, including 10 males, 16 females, and 1 fetus of undetermined sex (Table 1). Of these, 20 animals died from causes unrelated to cardiovascular disease or pathology including placental infarction, endometriosis, arthritis, amyloidosis, chronic enterocolitis, gastritis, gastroenteritis, colitis, or ear infection. The remaining 7 animals had histologic evidence of myocarditis and were selected to compare heart tissues with lower and higher histopathology scores (i.e., not randomly selected). Heart tissues from 3 of the animals with no indications of cardiovascular disease or lesions were

examined after being administered dextran to identify long-lived macrophages by immunofluorescence staining.[32] Dextran (Dextran, Amino, 10,000 MW; Thermo Fisher Scientific, Waltham, MA; D1860) was inoculated by intravenous (75–150 mg/kg), aerosol (100–300 μ;g/kg), and intrathecal (1–2.5 mg/kg) routes.

2.2 Tissue processing, histopathology, and immunofluorescence staining

Tissues from heart (apex, interventricular septum, left and right atria, papillary muscles, and ventricles) and skeletal muscle (middle section of *rectus femoris*) were collected at necropsy, fixed in Z-Fix (buffered zinc formalin fixative; Anatech Ltd., Battle Creek, MI), and embedded in paraffin. Longitudinal tissue sections of 5-μ;m thickness were stained with H&E on a Leica AutoStainer XL (Leica Biosystems, Buffalo Grove, IL). For immunofluorescence staining, 5-μ;m thick tissue sections were deparaffinized with xylene, rehydrated in graded ethanol and deionized water, microwaved for 20 min with 0.1% Tween 20 in 10% high pH solution (Vector Laboratories; Burlingame, CA; cat. # H3301), and transferred to a hot 2% antigen unmasking solution (Vector Laboratories; cat. # H3300) for 30 min. Tissue sections were then incubated for 5 min in 0.05% Sudan Black B, blocked with 10% normal goat serum (Thermo Fisher Scientific; cat. # 16210–064) for 40 min, and incubated for 1 h at room temperature with primary antibody followed by incubation with secondary antibody (Table 2) for 30 min. Antibodies were diluted with 0.2% cold water fish skin gelatin (FSG; Millipore-Sigma, St. Louis, MO; cat. # G-7765) in PBS and slides were washed with PBSFSG-Triton 100 (Millipore-Sigma; cat. # X-100) twice for 10 min after each antibody incubation. Then, nuclei were stained with 0.2 μ;g/mL DAPI dilactate (Thermo Fisher Scientific; cat. # D3571) in PBS for 10 min at room temperature. Slides were washed again and cover-slipped using a fluorescence mounting medium prepared by mixing 2.4 g Mowiol 4–88 (Calbiochem, Darmstadt, Germany, 475904) in 6 g glycerol (Millipore-Sigma; cat. # G6279) followed by addition of 6 mL double-distilled H_2O. After incubation on a shaker for 4–5 h at room temp, 12 mL of 0.2 M Tris buffer (pH 8.5; Thermo Fisher Scientific; cat. # BP152) was added followed by heating at 50°C for 10 min and addition of 0.45 g 1,4-Diazabicyclo[2.2.2]octane (DABCO; Millipore-Sigma, cat. # D27802) to reduce fading. Prior to use, the mounting medium was centrifuged at 5,000 × *g* for 15 min and supernatant medium was supplied at room temperature to avoid formation of air bubbles.

2.3 Histopathology scoring

Tissue sections from each animal processed for H&E and immunofluorescent antibody staining were examined by 2 pathologists and scored for lesions as previously described with slight modification[33] and as represented in Supplementary Fig. 1. Tissue scores were: 0 = normal tissue with no inflammatory infiltrate (Supplementary Fig. 1A), 1 = minimal with 1–5 mononuclear cells/HPF (40× objective lens) and/or 1–2 foci/per section (Supplementary Fig. 1B), 2 = mild with 6–20 mononuclear cells/HPF and/or 3–5 foci/section (Supplementary Fig. 1C), 3 = moderate with more than 20 mononuclear cells/HPF and/or 6–20 foci/section (Supplementary Fig. 1D), and 4 = severe inflammation with multifocal to coalescent inflammatory infiltrates (Supplementary Fig. 1E–H). Occasionally, the histolopathology scores were adjusted to accommodate lesions of hemorrhage

(Supplementary Fig. 1E), necrosis (Supplementary Fig. 1G), myocardial degeneration (Supplementary Fig. 1I), or bacterial abscess (Supplementary Fig. 1H).

2.4 Quantitative image assessments

Photomicrographs were taken from 11 random HPFs/tissue section (i.e., 1 HPF = 0.09048 mm^2 so 11 HPFs = 1 mm^2) from H&E slides used to complete histopathological evaluations and fluorescence-stained slides to perform macrophage phenotyping and detection of T- and B-cells, using a 40× objective of a Leica DMRE microscope (Leica Microsystems; Wetzlar, Germany) and Nuance FX camera (PerkinElmer; Waltham, MA). Images containing large blood vessels were excluded from the study. The percentage of positive cells for each biomarker was calculated by using the total number of DAPI-stained nucleated cells as the denominator. Mean fluorescence intensity of cells stained with individual fluorochromes was measured and compared using normalized values for each fluorochrome calculated as counts/gain*binning2*exposure time*2bit depth. Images were analyzed with InForm (PerkinElmer) and Fiji software.[34]

2.5 Statistical analyses

Mean values of results were assessed by unpaired *t* test for comparing 2 groups or 1-way ANOVA for comparing more than 2 groups that followed by Kruskal-Wallis post-test for pairwise comparisons. Spearman analysis was used for measuring correlations. $P < 0.05$ was considered statistically significant. Analyses and graphs were prepared using GraphPad Prism version 8.1.2 for Windows, GraphPad Software, La Jolla, CA (www.graphpad.com). Venn diagrams were generated with online software (https://omics.pnl.gov/software/venn-diagram-plotter; Pacific Northwest National Laboratory, United States Department of Energy) to illustrate the percent of macrophages expressing 2 biomarkers singly and in combination (i.e., CD163, HAM56, and/or CD206) relative to total heart cell nuclei.

3 RESULTS

3.1 Distribution and phenotype of macrophages in adult rhesus macaque heart tissues

In addition to muscle cells, normal heart tissue includes cells, such as macrophages, that participate in immune responses and tissue repair, and these cell functions may also contribute to tissue damage or disease over time. Thus, we initially evaluated the distribution of macrophages in relation to total number of cells (based on number of nuclei) in different areas of the heart from 3 adult rhesus macaques of 5.7, 6.7, and 11.8 years of age with histopathology scores of 0–2 (animals IP62, IB90, and EL85, respectively; Table 1). Cellularity ranged from 1374 ± 83 to 1782 ± 423/mm^2 among all the areas examined (Figs. 1A and B). There were no statistically significant differences in mean numbers of cells per area between regions of the heart. However, cellularity was slightly higher in the atrium than the ventricles and in the left side than right side (data not shown).

We then used 3 antibodies specific for CD163 (haemoglobin– haptoglobin scavenger receptor), HAM56 (macrophage marker), and CD206 (mannose receptor) (Table 2) to enumerate macrophages and their subsets in heart tissue of these 3 animals with relatively lower histopathology scores. Macrophages were readily detected within interstitial spaces

between myocytes (Fig. 1C). The distribution of nuclei, that is, cellularity (Fig. 1B) and average percentages of total macrophages detected with each antibody were similarly distributed throughout all areas of the heart (Fig. 1D) despite the low or sub-clinical inflammation scored in the left atrium of all 3 animals. The mean percentages of macrophages relative to total numbers of cells showed that the CD163-expressing subset of macrophages was the highest (1.6 ± 1.3–2.8 ± 1.3 with an overall mean for all areas being 2.4 ± 1.1), followed by HAM56-positive (1.3 ± 0.7–2.2 ± 1.1; mean of all areas = 1.9 ± 0.9) and CD206-positive (0.7 ± 0.8–1.5 ± 2.0; mean of all areas = 1.0 ± 1.0) macrophages in all cardiac anatomic locations. There were no significant differences between macrophage phenotype populations based on expression of combinations of CD163, HAM56, and CD206 in different anatomic locations examined. Most of the macrophages positive for HAM56 (i.e., 1.4 of 1.9%) or CD206 (0.8 of 1.0%) were also positive for CD163, while a smaller fraction of double-positive macrophages expressed HAM56 and CD206 (0.3 of 1.9% and 1.0%, respectively; Fig. 1E).

3.2 Cellularity in heart tissues of rhesus macaques at different ages

Next, we analyzed the cellularity in left or right ventricles from 21 animals ranging from fetal stage to 24 years of age with histopathology scores of 0–2. As shown in Fig. 2A (left graph), there was a significant correlation between declining numbers of cell nuclei/mm^2 area with increasing age that showed a dramatic decline early in life. We, thus, compared results by age groups (Fig. 2A right graph), which showed that there was a significantly higher mean number of cells/mm^2 (4313 ± 951) in heart tissue of fetus to 0.5-year-old macaques (n = 6) compared to that in heart tissues from macaques of 1.9–12 years of age (n = 8; 1641 ± 164) or 13–24 years of age (n = 7; 1325 ± 285). Representative images in Fig. 2B showed that the decrease in cellularity was associated with growth in heart myocyte size, as well as a slight increase of the intermyocyte spaces as animals became older.

3.3 Comparison of macrophage subsets in heart tissues from macaques of different ages

The percentages of macrophage populations were then examined in ventricle and atrium heart tissue sections from macaques of different ages that exhibited histopathology scores of 0–2. Results shown in Fig. 3A (left graph) demonstrated that there was a significantly higher mean percentage of CD163-staining macrophages in the group of animals aged 13–24 years old (n = 7; 3.8 ± 0.9) compared to that in animals aged 0–0.5 years old (n = 6; 1.8 ± 0.6). The percentage of CD163-positive macrophages also was higher in the older group compared to the 2- to 12-year-old animals (n = 5; 2.6 ± 0.6) but this difference did not reach statistical significance. The mean percent of HAM56-positive macrophages in the group of animals at 0–0.5 years of age was 0.9 ± 0.5 and increased to 2.1 ± 0.6 in the 2- to 12-year-old animals, while the percent of CD206-positive macrophages was 0.8 ± 0.3 in the very young group and similarly increased to 1.2 ± 0.6 in the 2- to 12-year-old animals. However, these changes were not statistically significant. Furthermore, the percentages of HAM56-positive (2.0 ± 1.2) and CD206-positive (1.2 ± 0.6) macrophages in the 13- to 24-year-old animals remained similar to that of the 2- to 12-year-old animals but with greater variability. Macrophages in the heart tissues also were quantitated based on tissue section area rather than as a percent of total cell numbers or nuclei (Fig. 3A, right graph). Interestingly, the mean number of CD163+ macrophages per mm^2 was higher in the youngest group of 0- to

0.5-year-old animals (67.9 ± 23.0) compared to those in heart tissues of the 2- to 12-year-old animals (44.0 ± 13.9) and 13- to 24-year-old animals (52 ± 21.14) despite the increasing mean percentages of macrophages in the older groups. Also, the absolute numbers of macrophages expressing CD163, HAM56, or CD206 per mm^2 were not statistically significantly different between age groups.

To better understand the increasing percentage of macrophages in heart tissues of the older group of animals, the phenotype and fluorescence intensity expression for each of the macrophage markers were compared. Among the macrophages in the animals aged 2–12 and 13–24 years old, over 80% of the HAM56-positive cells co-expressed CD163 (i.e., 1.7 of 2.1 = 80.95% and 2.0 of 2.1 = 95.24%, respectively) and over 90% of the CD206-positive macrophages co-expressed CD163 (i.e., 1.1 of 1.2 = 91.67% and 1.2 of 1.2 = 100%, respectively; Fig. 3B). There also was a higher proportion of CD163 single-positive macrophages in the fetus to 0.5-year-old group of animals compared to the younger and older adult groups of animals. Similar levels of cell fluorescence intensity for each of the 3 macrophage surface biomarkers were observed in heart tissues when comparing between the 2–12 and 13–24 year old groups (Fig. 3C). However, the mean fluorescence intensity was significantly lower for CD163-staining macrophages in heart tissue of the fetus to 0.5 year old animals (4.2 ± 2.4) compared to the 2- to 12-year-old animals (23.9 ± 9.3) and 13- to 24-year-old animals (27.3 ± 10.0). The mean fluorescence intensity of HAM56 was significantly higher in the animals aged 2–12 years (31.1 ± 7.8) than the youngest group of animals (10.9 ± 6.3) and was higher but more variable in the 13–24 year old animals (23.6 ± 18.1) that was not statistically significantly different. Mean fluorescence intensity for CD206 also was lower in the youngest group compared to the 2–12 and 13–24 year old animals but these comparisons were not statistically significantly different.

3.4 Distribution of lymphocytes in relatively healthy heart tissue of macaques at different ages

Lymphocytes found in heart tissue also may play a role in heart disease and aging.[35] Thus, we examined the distribution of CD3-positive T-cells and CD20-positive B-cells in relation to CD163-positive macrophages in rhesus macaque heart tissue with histopathology scores of 0–2. In heart tissues from animals of the 3 age groups, the mean percentages of CD3-positive and CD20-positive cells were significantly lower than of CD163-positive cells (Fig. 4B left graph). The average percent of B-cells was below 1% in each age group, but the percent of T-cells increased from 0.1 ± 0.1 in the group of fetus to 0.5 year old animals (n = 6) to 0.5 ± 0.3 in the 2- to 12-year-old animals (n = 5) and then to 0.8 ± 0.6 in the older group at 13–24 years of age (n = 7). There were similar trends in absolute numbers of CD3+ T-cells and CD20+ B-cells that also were lower than numbers of CD163+ macrophages in the 3 age groups (Fig. 4B right graph). Although the percentages of CD3-positive T-cells were not statistically significantly different between the 3 age groups, there was a statistically significant direct correlation between percentages of CD163-positive macrophages and CD3-positive T-cells (r = 0.510; P = 0.0362) (Fig. 4C) but not between absolute numbers of these 2 cell populations (not shown).

3.5 CD163 single-positive macrophages increase in heart tissues with clinical heart disease

Diseased heart tissue often is associated with an accumulation of inflammatory cells, including macrophages,[1,4,5] so we next examined the macrophage phenotype populations in heart tissue sections of rhesus macaques that were assigned pathology scores of 3–4 (Table 1; Supplementary Fig. 1). Heart tissues from 7 rhesus macaques exhibiting severe myocarditis were analyzed and compared with heart tissues from 9 animals of similar ages with histopathology scores of 0–2. Representative images of immunofluorescence-stained tissues showed the presence of more CD163-positive macrophages in the ventricles of heart tissue with higher histopathology scores of 3–4 than in heart tissue with a lower histopathology scores of 0–2 (Fig. 5A). A mean of 26.7% (± 14.6) CD163-positive macrophages was detected in ventricles of animals with pathology scores of 3–4, which was significantly higher than the mean of 2.9% (± 0.6) of CD163-positive macrophages detected in heart tissues with lower histopathology scores of 0–2 (Fig. 5B left graph). Similarly, there was a significantly higher mean absolute number of CD163+ macrophages per mm^2 area in animals with higher histopathology scores (618.5 ± 586.3) compared to those with lower histopathology scores (54.1 ± 21.7), as shown in Fig. 5B (right graph). Most of the CD163-positive macrophages co-expressed HAM56 in heart tissues with histopathology scores of 0–2 whereas CD163 single-positive macrophages predominated in heart tissues of animals with histopathology scores of 3–4 (Fig. 5C). Moreover, macrophages from heart tissues with histopathology scores of 3–4 exhibited lower cell fluorescence intensities for CD163 (13.4 ± 11.2) and HAM56 (12.1 ± 12.5) than those for CD163 (24.2 ± 11.1) and HAM56 (27.3 ± 9.0) from heart tissues with histopathology scores of 0–2 (Fig. 5D). This suggested that diseased heart tissue is comprised of more CD163 single-positive macrophages compared to a higher presence of macrophages that express both CD163 and HAM56 in relatively healthier heart tissue.

3.6 Macrophage distribution is similar in heart and skeletal muscles

Heart muscle and skeletal muscle are controlled by the autonomic and somatic nervous systems, respectively, but both are categorized as striated muscle.[36] So, we compared the cellularity and macrophage composition in tissue sections of heart ventricle ($n = 5$) and skeletal muscle (middle *rectus femoris*, $n = 3$) from animals aged 2–12 years with histopathology scores of 0–2 that were stained with H&E and DAPI. Representative images are shown in Fig. 6A, and quantification results plotted in Fig. 6B indicated that cellularity, or mean number of nuclei/mm^2, was significantly lower in skeletal muscle (586 ± 31) than in heart (1573 ± 139). Interestingly, among total macrophages, there were no significant differences between percentages of CD163-positive cells in skeletal muscle (2.7 ± 2.0) versus heart (2.6 ± 0.6) or HAM56-positive macrophages in skeletal muscle (1.7 ± 1.4) versus heart (2.4 ± 0.8) (Fig. 6C). In addition, the proportion of CD163-HAM56 double-positive cells was similar in both muscle tissues (Fig. 6D).

3.7 Long-lived macrophages in heart and skeletal muscle

We next examined heart and skeletal muscle for the presence of long-lived macrophages that incorporated and retained dextran. Dextran was inoculated 15–43 days prior to obtaining the

samples from 3 macaques aged 1.9, 2.9, and 5.7 years of age (animals KR74, KG16, and IM47, respectively; Table 1) with histopathology scores of 0–2. Heart and skeletal muscle tissues were stained with antibodies specific for dextran and the macrophage biomarkers CD163, HAM56, and CD206, as well as with DAPI to identify cell nuclei (Fig. 7). In heart tissue, means of 2.3% (± 1.3) macrophages stained positive for only CD163 and 2.0% (± 1.3) stained positive for both CD163 and dextran indicating that 46.5% of all CD163-positive macrophages in heart were long lived. In skeletal muscle, means of 0.8% (± 0.5) of macrophages stained positive for only CD163 and 2.7% (± 1.1) stained positive for both CD163 and dextran resulting in a higher percentage of 77.1% of CD163-positive macrophages in skeletal muscle that were long lived. Similarly, means of 1.6% (± 1.1) macrophages in heart tissue sections stained for only HAM56 and 1.2% (± 0.9) macrophages stained for both HAM56 and dextran, reflecting that 42.9% of this population of macrophages were long lived. In skeletal muscle, means of 2.0% (± 0.1) macrophages stained with HAM56 only and 2.2% (± 1.7) macrophages were positive for HAM56 and dextran, reflecting a majority or 53.0% of these macrophages that were longer lived. CD206-staining macrophages were not determined in skeletal muscle but in heart muscle, means of 0.3% (± 0.2) macrophages stained for CD206 only and 0.7% (± 0.6) macrophages stained for CD206 and dextran, suggesting that 70% of these CD206-positive macrophages appeared to be longer lived.

4 DISCUSSION

Immune cells of the heart participate in resistance to pathogens and tissue homeostasis but also play roles in pathogenesis of HIV infection, aging, and other conditions of risk for cardiovascular disease in humans. Rhesus macaques are similar in physiology to humans and, thus, serve as useful experimental models to study human disease, as well as to perform experimental procedures and repeated tissue samplings that may not be readily accomplished in humans. The purpose of this study was to characterize the macrophages in heart tissues of rhesus macaques with relatively normal to severe histopathology scores and ranging from fetal to older age. The rationale to focus on macrophages was that these cells function in innate immunity and homeostasis, but also may contribute to disease pathogenesis via inflammation and fibrosis.[15] Published reports primarily evaluated numbers of macrophages per microscopic field of view[35,37,38] and here, we also included enumerations of macrophages relative to total cell numbers (cellularity) in heart tissues from animals in different age groups. These results demonstrated that the overall cellularity (i.e., cell nuclei/mm^2) was similar throughout different areas of the heart in young adult animals with lower histopathology lesion scores of 0–2. Heart tissue cellularity was significantly higher in animals of fetal to 0.5 years (i.e., 6 months) of age compared to adult and older macaques. The increased cellularity, likely due to the smaller size of myocytes, facilitated the presence of more cells per area of tissue. With increasing age, myocyte size appeared to increase leading to reduce overall cellularity per field of view. Studies in mice indicated that numbers of cardiac myocytes are established by birth, further suggesting that the higher cellularity in the infant rhesus macaques related to smaller size rather than from proliferation of myocytes.[39]

Since heart tissue cellularity may affect macrophage analyses, the studies presented here included approaches to normalize the numbers of macrophages relative to the total numbers of cell nuclei per field of view. We first examined relatively healthy heart tissues based on the lower histopathology scores of 0–2 (Supplementary Fig. 1) to determine the basal distribution of macrophages. The distribution of macrophages in different regions of the heart was homogeneous, suggesting that examination of limited heart samples appears to reflect macrophage populations throughout the heart with the exception of specialized structures such as valves. As a result, the subsequent studies performed here relied on tissue samples available from atria and/or ventricles to compare the distribution of macrophage subpopulations from animals of different ages.

Overall, the highest percentages of macrophages in heart were positive for CD163, followed by expression of HAM56 and then CD206. This higher percentage of CD163-positive macrophages relative to total heart cells in the animals over 2 years of age was consistent with reports by others.[35] However, we did not observe a decrease of HAM56-expressing macrophages that was reported previously in older animals.[35] Instead, we found that while HAM56 cells were less than 1% of all cells in heart tissue from animals of prenatal to 6 months of age, these cells increased and remained stable in animals over 6 months of age. Cell fluorescence intensities of CD163 and HAM56 in heart tissue were lower in the younger animals and higher in the older animals. Thus, the lower percentage of macrophages observed in the youngest animals could be due to a lower number of positively staining macrophages relative to total cell nuclei or to a lower level of biomarker expression that may have been undetected by the immunofluorescence staining techniques used here.

The increased percentage of macrophages in heart tissue of animals over 6 months of age suggested that blood monocytes may traffic to heart tissue where they differentiate into tissue macrophages or that macrophages proliferate or self-renew within the heart.[40] In vivo thymidine analogue labeling using BrdU in macaques has been used to evaluate the kinetics, turnover, and phenotype of short-lived macrophages originating from the bone marrow.[11,41,42] Unincorporated BrdU has a short half-life in vivo and cells in the process of division incorporate this thymidine analogue which then can be detected by immunostaining. This approach determined that in lung, a high proportion of the interstitial macrophages divided recently and, thus, were considered to be shorter-lived.[11] To our knowledge, however, no studies have demonstrated that local proliferation was responsible for the higher percentage of macrophages in heart during aging, and thymidine analogue staining has not yet been performed to determine if shorter-lived or recently dividing macrophages exist in heart tissue. Results published by Bajpai et al, however, support the presence of recently dividing tissue macrophages based on gene expression data on left ventricular heart tissue specimens from patients with dilated and ischemic cardiomyopathies.[18] The investigators reported that the CCR2-positive rather than CCR-negative macrophages were more similar to blood monocytes and, thus, appeared to represent a recently recruited and shorter-lived population that would be analogous to the shorter-lived BrdU-labeled lung macrophages of our published studies.[11]

Conversely, longer-lived macrophages can be identified with preferential uptake and retention of in vivo administered amino dextran. Using this approach in a previous study,

alveolar macrophages, as opposed to interstitial macrophages of the lung, were characterized as being longer-lived and, thus, resident tissue macrophage.[11] In the present study, we observed that while cellularity was lower in skeletal muscle than in heart muscle, a predominant population of macrophages in both muscle tissues was longer-lived based on detection of internalized dextran. This was consistent with the reports by Epelman and colleagues who suggested that the origin of most heart macrophages in mice is embryonic, and under homeostasis, these macrophages are maintained through local proliferation without significant monocyte recruitment.[14] In the report by Bajpai et al comparing gene expression in macrophages from human heart failure patients, the CCR2-negative population appeared to represent such tissue-resident macrophages[18] and may resemble or be analogous to the dextran-retaining longer-lived macrophages reported here.

In the present study, macrophages also were observed at a higher percentage and number of total immune response cells compared to CD3 T-cells and CD20 B-cells in relatively healthy rhesus macaque heart tissue. While the percent of macrophages was higher in heart tissues of the older groups of animals, the percentages of B-cells remained fairly stable and in the older 13–24 year old monkeys, the percentage of T-cells increased slightly but at greater variability within this group. The lower percentage of T-cells measured in this report was consistent with a previous human study reporting 0–4 T-cells/mm^2 area of normal myocardium.[43] While T-cells increased significantly with aging in another study using macaques that may also have exhibited myocarditis,[35] our studies did suggest some increase with age although this was not statistically significant, possibly because the heart tissues selected for examination exhibited lower or relatively healthy histopathology scores. However, there was a significant direct correlation between percent of CD163-positive macrophages that increased with age, and percent of CD3 T-cells, suggesting a relationship between these cells during aging. Analyses on additional specimens from more animals may be needed to better understand shifts of T-cells in heart tissues of aging rhesus macaques.

Since macrophages regulate inflammation and may contribute to cardiovascular disease, we also examined heart tissues with higher histopathology scores for comparison to healthy heart tissues with relatively lower histopathology scores of 0–2 in animals over 0.5 years of age (Table 1). The percent of CD163-positive macrophages was significantly higher in the heart tissues with histopathology scores of 3–4 compared to those with lower scores, but was associated with lower mean fluorescence intensity levels. Under inflammatory conditions or heart tissue damage, monocytes appeared to be recruited to the heart to become tissue macrophages,[14,44] which may have accounted for the lower fluorescence intensity during cell differentiation.

5 CONCLUSION

These studies corroborate the presence of at least 2 distinct populations of macrophages in heart tissue of rhesus macaques and demonstrated that macrophages increase as a percent of total heart cells with aging and severity of (histo)pathologic condition. This rhesus macaque model is expected to contribute to continued studies focusing on functional roles of macrophages in heart tissues to address mechanisms of homeostasis, as well as pathogenesis in cardiovascular disease for developing intervention strategies to ameliorate disease.

Supplementary Material

Refer to Web version on PubMed Central for supplementary material.

ACKNOWLEDGMENTS

The authors gratefully acknowledge support from the National Institutes of Health including AI097059, HL125054, HL139278, AI110163, AG052349, and AI116198, as well as the base grant P51OD011104 to the Tulane National Primate Research Center. D.P. was supported by T32 OD011124. We would also like to thank Ms. Lifang Nieburg and Mr. Maurice Duplantis for assistance with necropsies and sample collections, as well as Ms. Carol Coyne and Ms. Rachel Silvestri for help with histological processing and tissue section preparation. We are appreciative to Dr. Xiaolei Wang for sharing samples from infants, Mr. Maciej Zerkowski at PerkinElmer, Inc. for the guidance with image analysis, and the TNPRC animal care personnel for the excellent veterinary service support. Finally, we would like to acknowledge the excellent technical assistance from Ms. Erin Haupt, Ms. Toni Penney, Ms. Edith Walker, and Ms. Nadia Slisarenko.

REFERENCES

1. Caforio AL, Pankuweit S, Arbustini E, et al. Current state of knowledge on aetiology, diagnosis, management, and therapy of myocarditis: a position statement of the european society of cardiology working group on myocardial and pericardial diseases. Eur Heart J. 2013;34:2636–2648. [PubMed: 23824828]
2. Chamanza R, Parry NM, Rogerson P, Nicol JR, Bradley AE. Spontaneous lesions of the cardiovascular system in purpose-bred laboratory nonhuman primates. Toxicol Pathol. 2006;34:357–363. [PubMed: 16844663]
3. Magnani JW, Dec GW. Myocarditis: current trends in diagnosis and treatment. Circulation. 2006;113:876–890. [PubMed: 16476862]
4. Azzawi M, Kan SW, Hillier V, Yonan N, Hutchinson IV, Hasleton PS. The distribution of cardiac macrophages in myocardial ischaemia and cardiomyopathy. Histopathology. 2005;46:314–319. [PubMed: 15720417]
5. Baughman KL. Diagnosis of myocarditis: death of Dallas criteria. Circulation. 2006;113:593–595. [PubMed: 16449736]
6. Shanes JG, Ghali J, Billingham ME, et al. Interobserver variability in the pathologic interpretation of endomyocardial biopsy results. Circulation. 1987;75:401–405. [PubMed: 3802444]
7. Frangogiannis NG. The immune system and cardiac repair. Pharmacological Res. 2008;58:88–111.
8. Yearley JH, Pearson C, Shannon RP, Mansfield KG. Phenotypic variation in myocardial macrophage populations suggests a role for macrophage activation in SIV-associated cardiac disease. AIDS Res Hum Retrovirus. 2007;23:515–524.
9. van Furth R, Cohn ZA, Hirsch JG, Humphrey JH, Spector WG, Langevoort HL. The mononuclear phagocyte system: a new classification of macrophages, monocytes, and their precursor cells. Bull World Health Org. 1972;46:845–852. [PubMed: 4538544]
10. Varga T, Mounier R, Patsalos A, et al. Macrophage PPARgamma, a lipid activated transcription factor controls the growth factor gdf3 and skeletal muscle regeneration. Immunity. 2016;45: 1038–1051. [PubMed: 27836432]
11. Cai Y, Sugimoto C, Arainga M, Alvarez X, Didier ES, Kuroda MJ. In vivo characterization of alveolar and interstitial lung macrophages in rhesus macaques: implications for understanding lung disease in humans. J Immunol. 2014;192:2821–2829. [PubMed: 24534529]
12. Laskin DL, Weinberger B, Laskin JD. Functional heterogeneity in liver and lung macrophages. J Leukoc Biol. 2001;70:163–170. [PubMed: 11493607]
13. Schneberger D, Aharonson-Raz K, Singh B. Monocyte and macrophage heterogeneity and Toll-like receptors in the lung. Cell Tissue Res. 2011;343:97–106. [PubMed: 20824285]
14. Epelman S, Lavine KJ, Beaudin AE, et al. Embryonic and adult-derived resident cardiac macrophages are maintained through distinct mechanisms at steady state and during inflammation. Immunity. 2014;40: 91–104. [PubMed: 24439267]

15. Epelman S, Lavine KJ, Randolph GJ. Origin and functions of tissue macrophages. Immunity. 2014;41:21–35. [PubMed: 25035951]
16. Lavine KJ, Epelman S, Uchida K, et al. Distinct macrophage lineages contribute to disparate patterns of cardiac recovery and remodeling in the neonatal and adult heart. Proc Natl Acad Sci USA. 2014;111: 16029–16034. [PubMed: 25349429]
17. Molawi K, Wolf Y, Kandalla PK, et al. Progressive replacement of embryo-derived cardiac macrophages with age. J Exp Med. 2014;211:2151–2158. [PubMed: 25245760]
18. Bajpai G, Schneider C, Wong N, et al. The human heart contains distinct macrophage subsets with divergent origins and functions. Nat Med. 2018;24:1234–1245. [PubMed: 29892064]
19. Twum DYF, Burkard-Mandel L, Abrams SI. The Dr. Jekyll and Mr. Hyde complexity of the macrophage response in disease. J Leuko Biol. 2017;102:307–315. [PubMed: 28319464]
20. Ortiz AM, DiNapoli SR, Brenchley JM. Macrophages are pheno-typically and functionally diverse across tissues in simian immunodeficiency virus-infected and uninfected asian macaques. J Virol. 2015;89:5883–5894. [PubMed: 25787286]
21. Wang C, Yu X, Cao Q, et al. Characterization of murine macrophages from bone marrow, spleen and peritoneum. BMC Immunol. 2013;14:6. [PubMed: 23384230]
22. Prabhu SD. Cytokine-induced modulation of cardiac function. Circ Res. 2004;95:1140–1153. [PubMed: 15591236]
23. Epelman S, Liu PP, Mann DL. Role of innate and adaptive immune mechanisms in cardiac injury and repair. Nat Rev Immunol. 2015;15:117–129. [PubMed: 25614321]
24. Perdiguero EG, Geissmann F. The development and maintenance of resident macrophages. Nat Immunol. 2016;17:2–8. [PubMed: 26681456]
25. Varol C, Mildner A, Jung S. Macrophages: development and tissue specialization. Ann Rev Immunol. 2015;33:643–675. [PubMed: 25861979]
26. Ma Y, Mouton AJ, Lindsey ML. Cardiac macrophage biology in the steady-state heart, the aging heart, and following myocardial infarction. Transl Res. 2018;191:15–28. [PubMed: 29106912]
27. Messaoudi I, Estep R, Robinson B, Wong SW. Nonhuman primate models of human immunology. Antioxid Redox Signal. 2011;14:261–273. [PubMed: 20524846]
28. Yuan Q, Zhou Z, Lindell SG, et al. The rhesus macaque is three times as diverse but more closely equivalent in damaging coding variation as compared to the human. BMC Genet. 2012;13:52. [PubMed: 22747632]
29. Cai Y, Sugimoto C, Arainga M, et al. Preferential destruction of interstitial macrophages over alveolar macrophages as a cause of pulmonary disease in Simian immunodeficiency virus-infected rhesus macaques. J Immunol. 2015;195:4884–4891. [PubMed: 26432896]
30. Cai Y, Sugimoto C, Liu DX, et al. Increased monocyte turnover is associated with interstitial macrophage accumulation and pulmonary tissue damage in SIV-infected rhesus macaques. J Leukoc Biol. 2015;97: 1147–1153. [PubMed: 25780057]
31. Council NR. Guide for the Care and Use of Laboratory Animals: Eighth Edition. Washington, D.C.: The National Academies Press; 2011.
32. Mowry RW, Millican RC. A histochemical study of the distribution and fate of dextran in tissues of the mouse. Am J Pathol. 1953;29: 523–545. [PubMed: 13040491]
33. Dunn ME, Coluccio D, Zabka TS, et al. Myocardial mononuclear cell infiltrates are not associated with increased serum cardiac troponin I in cynomolgus monkeys. Toxicol Pathol. 2012;40:647–650. [PubMed: 22298795]
34. Schindelin J, Arganda-Carreras I, Frise E, et al. Fiji: an open-source platform for biological-image analysis. Nat Meth. 2012;9:676–682.
35. Macri SC, Bailey CC, de Oca NM, et al. Immunophenotypic alterations in resident immune cells and myocardial fibrosis in the aging rhesus macaque (*Macaca mulatta*) heart. Toxicol Pathol. 2012;40:637–646. [PubMed: 22328408]
36. Brown TA. Physiology. St. Louis, MO: Elsevier; 2011:288.
37. Azzawi M, Hasleton PS, Kan SW, Hillier VF, Quigley A, Hutchinson IV. Distribution of myocardial macrophages in the normal human heart. J Anatomy. 1997;191(Pt 3):417–423.

38. Grasmeyer S, Oswald S, Madea B. Quantification of leucocytes, T-lymphocytes and macrophages in autoptical endomyocardial tissue from 56 normal human hearts during the first year of life. Forensic Sci Int. 2016;262:108–112. [PubMed: 26978534]

39. Alkass K, Panula J, Westman M, Wu TD, Guerquin-Kern JL, Bergmann O. No evidence for cardiomyocyte number expansion in preadolescent mice. Cell. 2015;163:1026–1036. [PubMed: 26544945]

40. Ensan S, Li A, Besla R, et al. Self-renewing resident arterial macrophages arise from embryonic CX3CR1(+) precursors and circulating monocytes immediately after birth. Nat Immunol. 2016;17: 159–168. [PubMed: 26642357]

41. Hasegawa A, Liu H, Ling B, et al. The level of monocyte turnover predicts disease progression in the macaque model of AIDS. Blood. 2009;114:2917–2925. [PubMed: 19383966]

42. Sugimoto C, Hasegawa A, Saito Y, et al. Differentiation kinetics of blood monocytes and dendritic cells in macaques: insights to understanding human myeloid cell development. J Immunol. 2015;195: 1774–1781. [PubMed: 26179903]

43. Feeley KM, Harris J, Suvarna SK. Necropsy diagnosis of myocarditis: a retrospective study using CD45RO immunohistochemistry. J Clin Pathol. 2000;53:147–149. [PubMed: 10767832]

44. Sager HB, Hulsmans M, Lavine KJ, et al. Proliferation and recruitment contribute to myocardial macrophage expansion in chronic heart failure. Circ Res. 2016;119:853–864. [PubMed: 27444755]

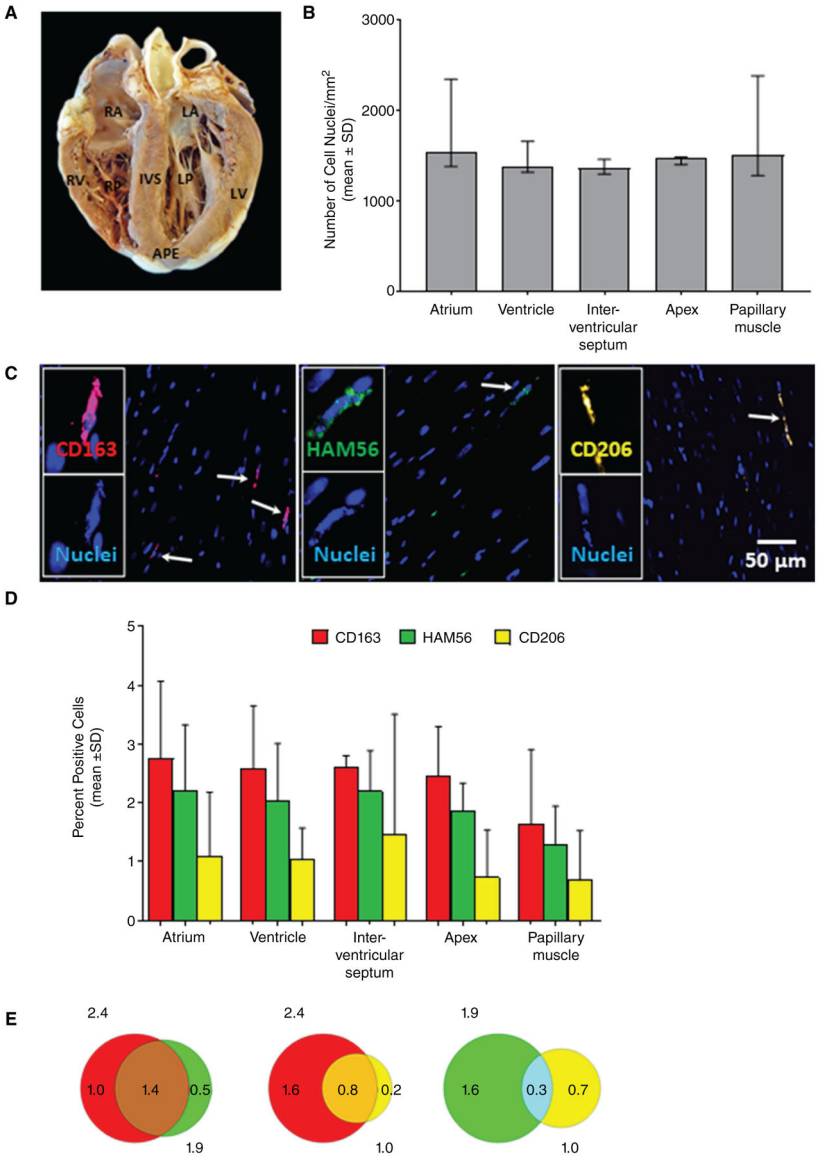

FIGURE 1. Macrophages are similarly and consistently distributed throughout various regions of the heart with low histopathology scores in adult rhesus macaques.

Heart tissue sections obtained at necropsy from 3 adult rhesus macaques (ages 5.7, 6.7, and 11.8 years; animals IP62, IB90, and EL85, respectively) with histopathology scores of 0–2 were evaluated for comparisons of tissue cellularity and macrophage distribution. (**A**) An image of rhesus macaque heart (courtesy of Ms. Lifang Nieburg) demonstrates areas from which samples were examined that included the apex (APE), interventricular septum (IVS), left atrium (LA), left papillary muscle (LPM), left ventricle (LV), right atrium (RA), right papillary muscle (RP), and right ventricle (RV). (**B**) Eleven random fields of view (equivalent to 1 mm^2) from each region of the heart of the 3 animals were evaluated and the mean numbers of cell nuclei per mm^2 section (± SD) were plotted. (**C**) Representative immunofluorescence images of macrophages demonstrate expression of biomarkers CD163, HAM56, and CD206. Staining with DAPI identifies cell nuclei. (**D**) Mean percentages (± SD) of macrophage populations among all nucleated cells of the designated regions of the

heart were plotted after viewing 11 fields of view per region of the heart per animal. (**E**) Venn diagrams illustrate the proportions of macrophages co-expressing sets of 2 biomarkers as percentages of cell nuclei in all regions of the heart. Biomarkers examined are the same as shown for the legend in Panel D. One-way ANOVA was used to test overall significance and if significant, Kruskal-Wallis post-test then was applied for pairwise comparisons. $P < 0.05$ was considered statistically significant

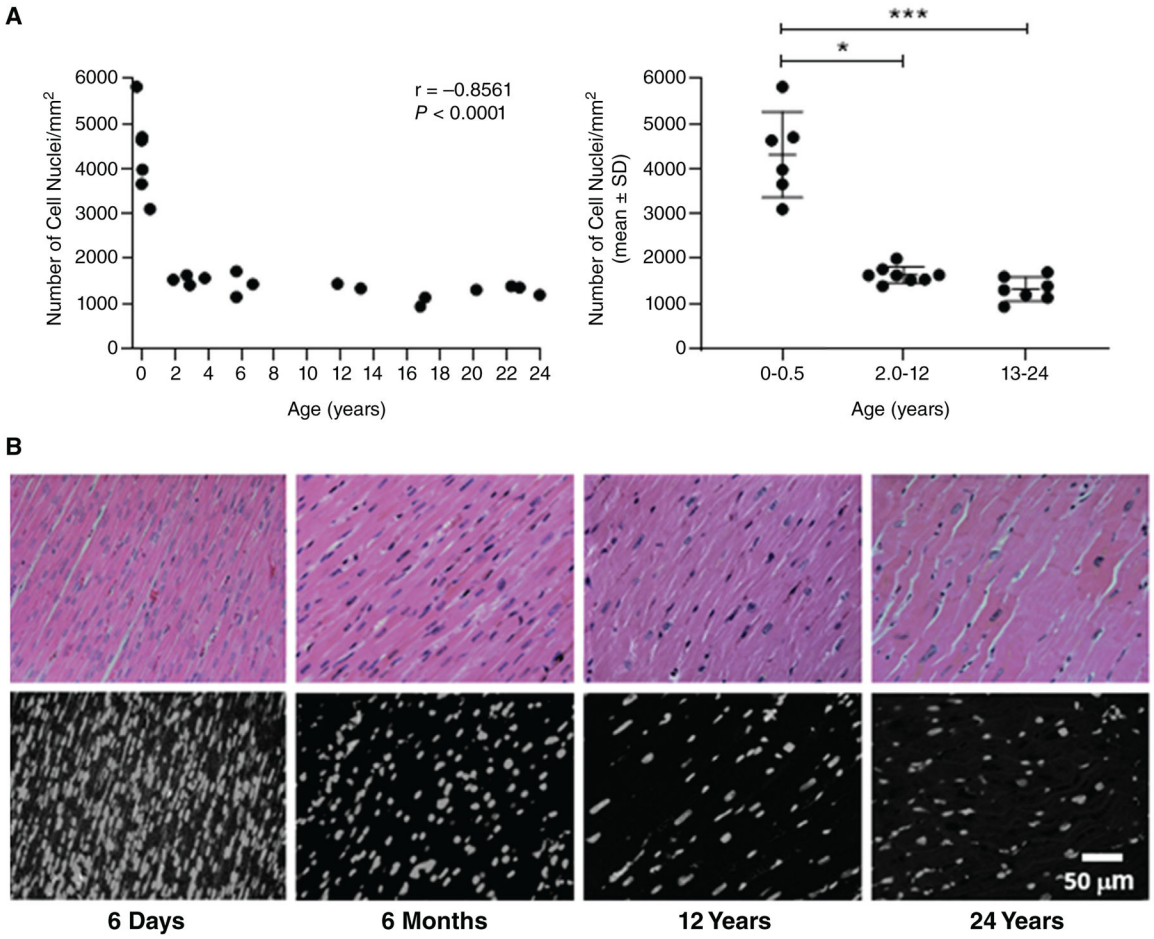

FIGURE 2. Cell density in heart is greater in very young rhesus macaques compared to adults.

(**A**) The numbers of cell nuclei were counted in left/right ventricle tissue sections from rhesus macaques with histopathology scores of 0–2. The graph on the left compares numbers of cell nuclei/mm^2 versus age in years using Spearman correlation analysis. The graph on the right compares mean numbers of cell nuclei per mm^2 area (± SD) by age group. One-way ANOVA was measured ($P < 0.0001$) followed by Kruskal-Wallis post-test for pairwise comparisons. $P < 0.05$ was considered statistically significant; *$P < 0.05$, ***$P < 0.001$. (**B**) Representative tissue section images of left or right ventricles with histopathology scores of 0–2 from rhesus macaques were stained with H&E (upper panel) or DAPI (lower panel)

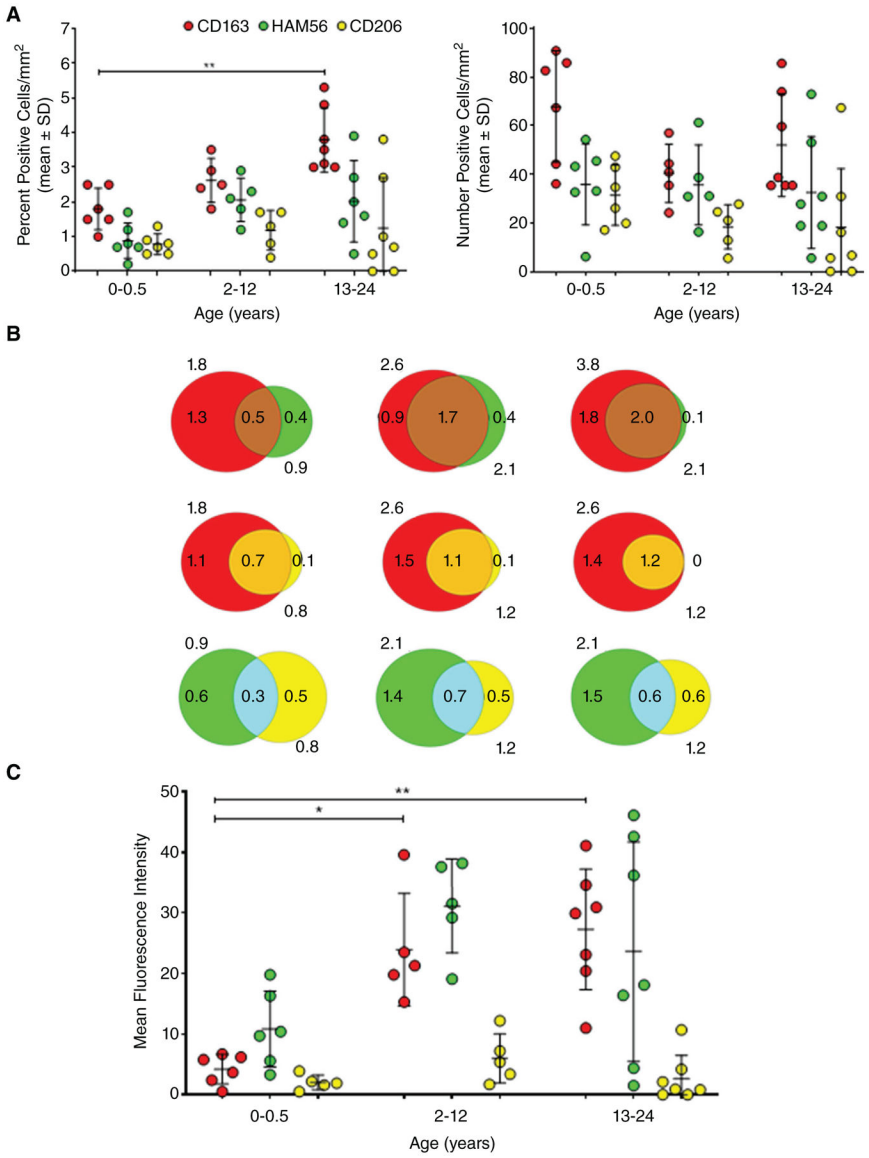

FIGURE 3. Percentages of macrophage subpopulations in the heart differ between age groups of rhesus macaques.

Ventricle and atrium tissues of animals with lower histopathology scores (0–2) were processed, immunostained for macrophages expressing CD163, HAM56, and CD206, and imaged by fluorescence microscopy. (**A**) Macrophages expressing CD163, HAM56, and CD206 were counted as a percent of DAPI-stained cell nuclei (left graph) and as number of cells/mm^2 (right graph). One-way ANOVA of macrophage percentages indicated statistical significance ($P < 0.0001$) and Kruskal-Wallis post-test then was applied for pairwise comparisons; $^{**}P < 0.01$. (**B**) Venn diagrams illustrate percentages of macrophage subpopulations (see legend of Panel A) and co-expression of 2 biomarkers within each age group based on cellularity (cell nuclei). (**C**) Mean cell fluorescence intensity levels (± SD) were plotted for each macrophage biomarker (per legend in panel A) in the ventricle and atrium heart tissues of macaques from the 3 age groups. One-way ANOVA was performed ($P < 0.0001$) and Kruskal-Wallis post-test was performed for pairwise comparisons; $^{*}P <$

0.05, $^{**}P < 0.01$. $P < 0.05$ was considered statistically significant [Correction added on 4 October 2019, after first online publication: Y-axis in figure 3A has been corrected from "Number Positive Cells/mm^2" to "Percent Positive Cells/mm^2"]

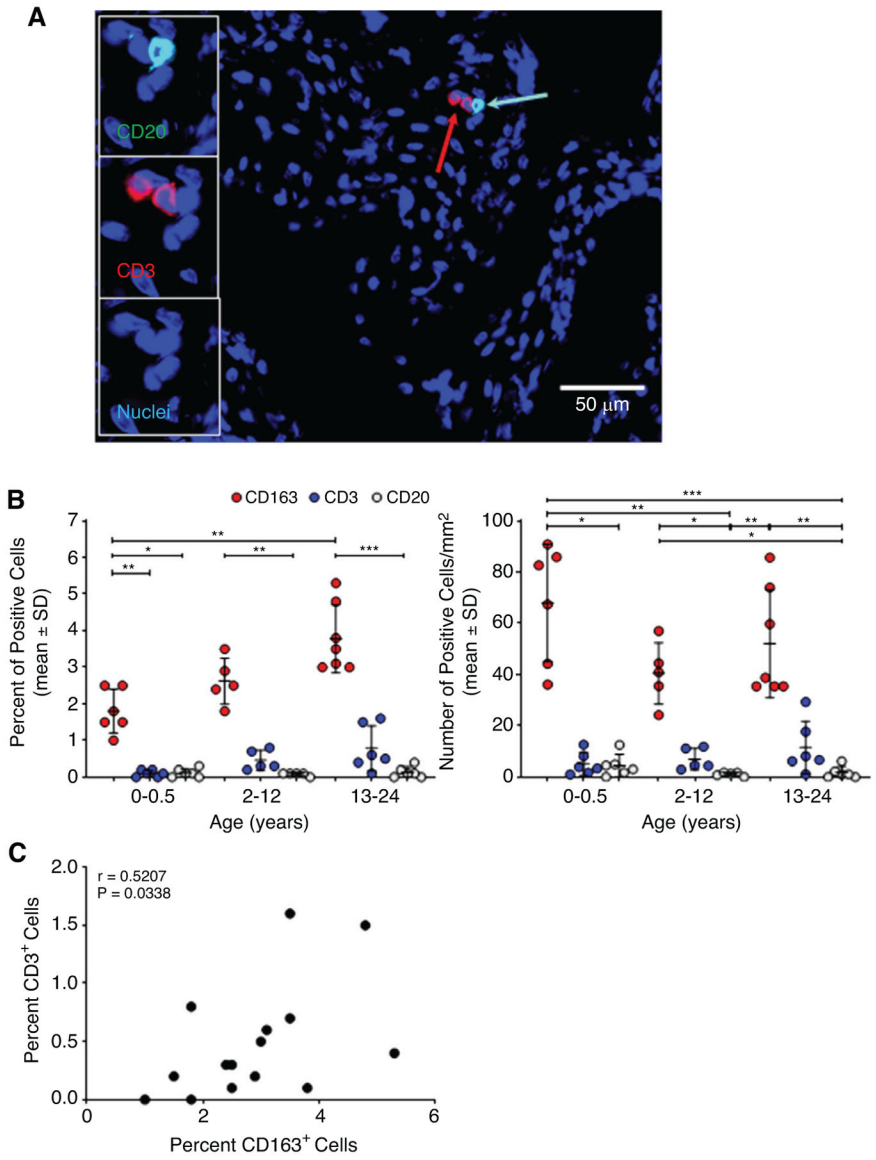

FIGURE 4. Percentages of lymphocytes in heart tissue are higher in older groups of rhesus macaques.

Ventricle and atrium tissue sections from rhesus macaques with histopathology scores of 0–2 were stained for cells expressing CD3 (T lymphocytes), CD20 (B lymphocytes), CD163 (macrophages), and DAPI (cell nuclei) and viewed by fluorescence microscopy. (**A**) A representative fluorescence microscopy image demonstrates detection of T- (red arrow) and B-cells (turquoise arrow). (**B**) Mean percentages in relation to total cell nuclei (left graph) and numbers/mm^2 (right graph) of macrophages, T-, and B-cells (± SD) among animals in each age group were plotted. One-way ANOVA was performed ($P < 0.0001$) followed by Kruskal-Wallis post-test for pairwise comparisons; *$P < 0.05$, **$P < 0.01$, ***$P < 0.01$, ****$P < 0.0001$. (**C**) Spearman correlation analysis was performed to compare the percent of CD3-positive T-cells in relation to percentages of CD163-positive macrophages per tissue section of each animal. $P < 0.05$ was considered statistically significant

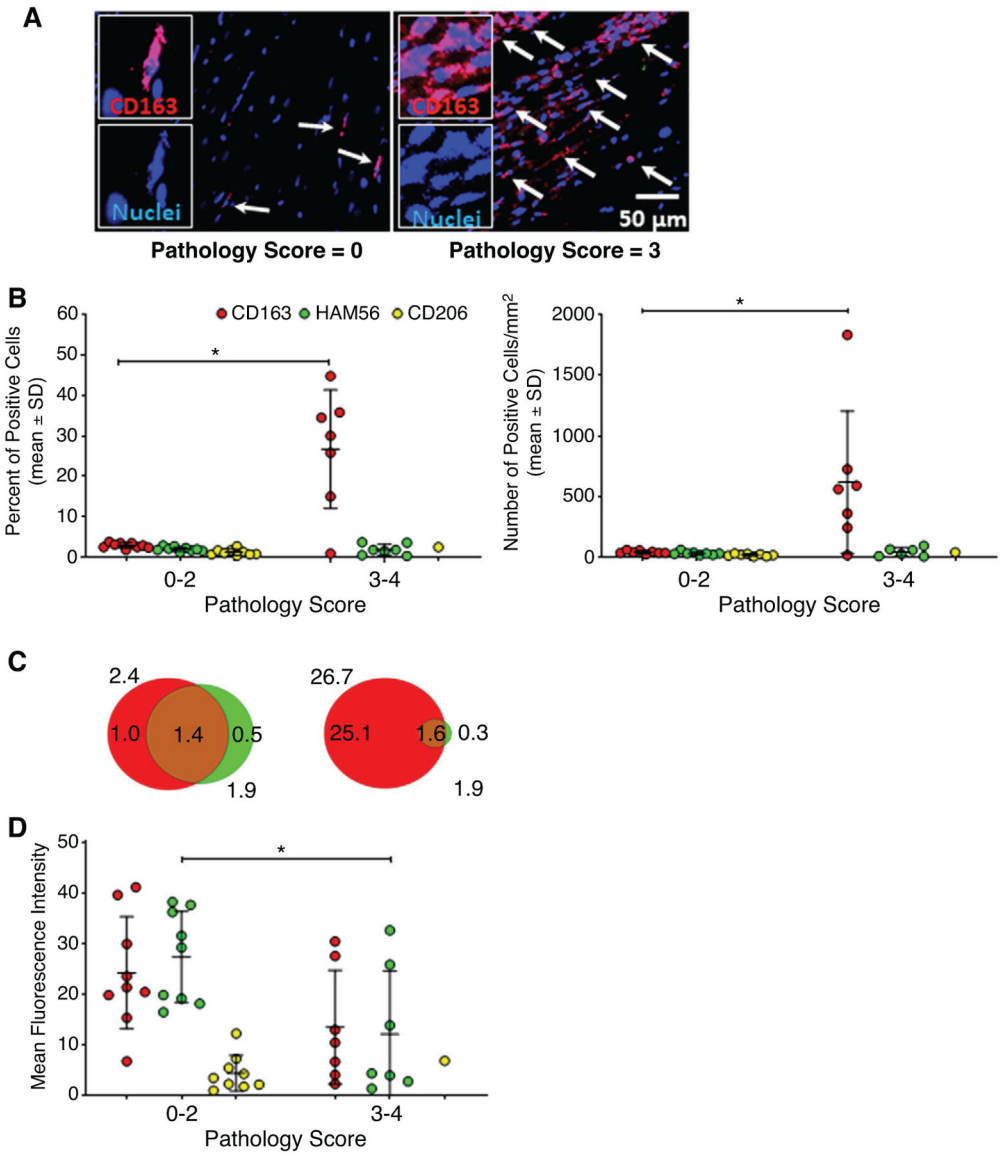

FIGURE 5. Macrophage are higher by percentage and number in animals exhibiting severe histopathology scores.

Heart tissue sections were examined from rhesus macaques exhibiting lower histopathology scores of 0–2 (0.5–17.1 years old) or higher histopathology scores of 3–4 (3.6–19.4 years old). Immunofluorescence microscopy was applied to detect macrophages expressing CD163, HAM56, and CD206, as well as DAPI-staining nucleated cells. (**A**) Representative fluorescence microscopy images compare detection of CD163+ macrophages (red stain indicated by white arrows) in heart tissue of 2 adult animals with a lower (left panel) and higher histopathology score (right panel). (**B**) The mean percentages of macrophages expressing CD163, HAM56, and CD206 in relation to cell nuclei (left graph) and absolute numbers/mm^2 (right graph) were plotted from animals with relatively lower and higher histopathology scores. One-way ANOVA was performed ($P < 0.0001$) followed by Kruskal-Wallis post-test for pairwise comparisons. *$P < 0.05$. (**C**) Venn diagrams illustrate the percentage of macrophages expressing CD163, HAM56, or both (overlapping) biomarkers

among total cell nuclei as indicated in the legend of Panel B. (**D**) Cell fluorescence intensities (mean ± SD) were plotted for macrophages expressing each biomarker (see legend in panel B) per animal grouped by lower (0–2) or higher (3–4) histopathology scores. Comparisons between groups were measured by one-way ANOVA ($P = 0.0002$) followed by Kruskal-Wallis post-test for pairwise comparisons; *$P < 0.05$. $P < 0.05$ was considered statistically significant

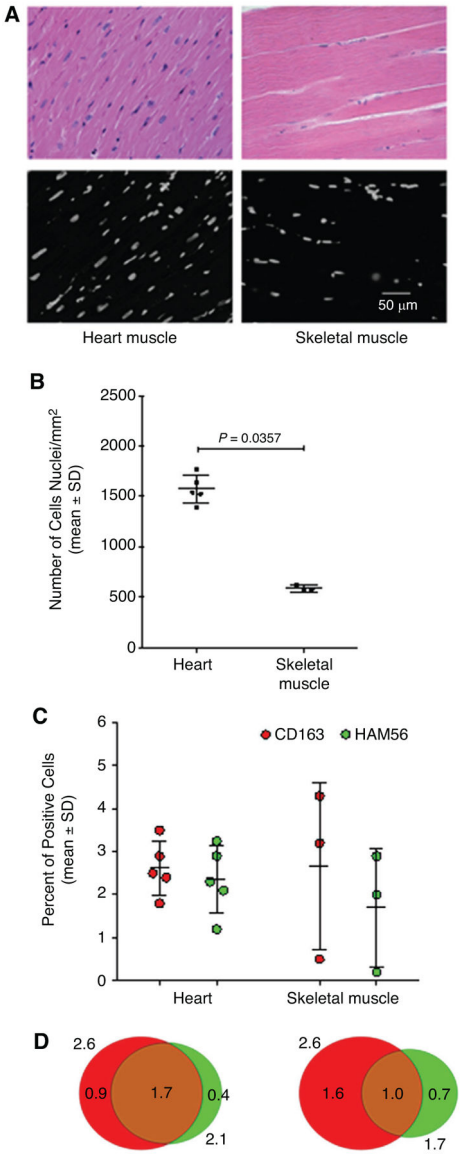

FIGURE 6. Greater cell density but similar macrophage percentages are observed in heart tissues with histopathology scores of 0–2 compared to skeletal muscle of adult rhesus macaques.

Heart ventricle and skeletal muscle (*rectus femoris*) tissues were examined from rhesus macaques aged 2–12 years old that exhibited relatively lower heart tissue histopathology scores of 0–2. (**A**) Representative images are shown of heart ventricle muscle and skeletal muscle stained with H&E (upper panel) or DAPI (lower panel). (**B**) The mean numbers of DAPI-stained cell nuclei per mm^2 area of each muscle tissue per animal (± SD) were plotted. Unpaired *t* test was performed and $P < 0.05$ was considered statistically significant. (**C**) Immunostaining and fluorescence microscopy were used to count CD163+ and HAM56+ macrophages in heart and skeletal muscle as a percent of DAPI-stained nucleated cells. By one-way ANOVA, there was no statistically significant difference between groups. $P < 0.05$ was considered statistically significant. (**D**) Venn diagrams illustrate the percentages of macrophages expressing CD163, HAM56, or both biomarkers (as indicated

in the legend of Panel C) in relation to total nucleated cells of heart (left) and skeletal muscle (right)

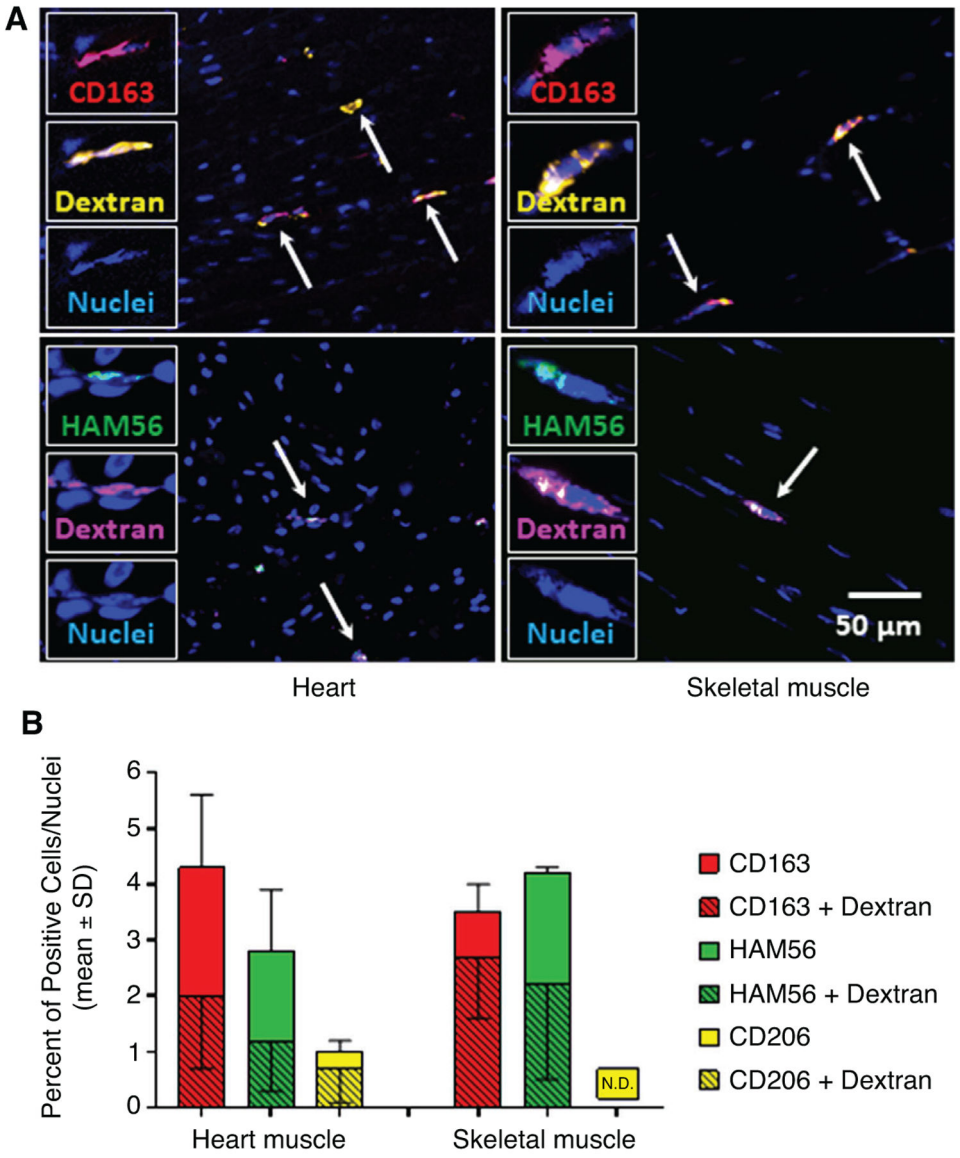

FIGURE 7. High proportions of macrophages in heart and skeletal muscle retained dextran and are considered long-lived.

Tissues were obtained from 3 rhesus macaques aged 1.9, 2.9, and 5.7 years of age (animals KR74, KG16, IM47, respectively) with low histopathology scores (0–2) in heart tissue and that had been administered dextran 15– 43 days earlier as described in the Materials and Methods. Heart ventricle and skeletal muscles were processed for immunostaining and fluorescence microscopy to detect macrophages expressing CD163, HAM56, and CD206 in conjunction with those that incorporated and retained dextran. (**A**) Representative images are shown for heart (left) and skeletal muscle (right) depicting macrophages that co-stained for dextran and CD163 (arrows) in the upper panels or dextran and HAM56 (arrows) in the lower panels. (**B**) The mean percentages of macrophages expressing each biomarker in relation to total number of nuclei (± SD) for each tissue site were plotted and the mean

proportions (± SD) of these cells that co-expressed staining for dextran were shown with black cross-hatch. N.D. = not determined

TABLE 1

Animals used in the study

			Histopathology scores of heart and skeletal muscle								Tissues used			
Animal	**Age (years)**	**Sex**	**LV**	**RV**	**LA**	**RA**	**APE**	**IVS**	**RECTF**	**Pathologic conditions**	**Heart**	**Skeltal muscle**	**Heart ventricle muscle**	**Dextran Inoc.**
LK92	Firsst trimester	UD	0						0	Maternal death	x	x		
LJ57	Third trimester	M	0			0				Placental infarction	x			
LJ55	Term	F	0			0				In utero bacterial pneumonia	x			
LK61	0.02	F	0	0		1				Epidermitis, vaccine control	x			
LK36	0.04	M	0	0		0				No lesions, vaccine study	x			
LI01	0.5	F	0	0		0				Generalized lymphoid hyperplasia, vaccine study	x			
KR74	1.9	M	1			0			0	Hydrocephalus	x	x	x	x
KL42	2.7	M	0	0		0			0	Colitis, splenic hyperplasia	x	x		
KG16	2.9	M	0	0		0			0	Encephalomalacia	x	x	x	x
K539	3.57	M	4							Bacterial myocarditis with abscesses	x			
KA51	3.8	M	0			0			0	Clinical encephalopathy	x	x		
D469	5.5	F	3							Bacterial myocarditis	x			
IM47	5.7	F	2	1		0			0	Lymphoid hyperplasia and dysplasia	x		x	x
IP62	5.7	F	1	0	1	0	1	0		Chronic gastroenterocolitis	x			
IB90	6.7	M	0	0	2	4	0	0		Chronic gastroenteritis	x			
F442	10	F	3							Myocarditis, etiology unknown	x			
EL85	11.8	F	0	0	1	0	1	0		Chronic gastritis	x			
CE23	12.7	F	4							Bacterial epicarditis and myocarditis	x			
DR52	13.2	F	0			1				Chronic dermatitis	x			
N702	14.7	F	3							Myocarditis and fibrosis	x			
CE12	16.8	F	2				2			Chronic otitis media	x			
DB52	17.1	M	1							Degenerative joint disease	x			
D826	19.4	F	3							Myocarditis, heart failure	x			
P202	20.2	M	1							Chronic enterocolitis, chronic myocarditis	x			
IR91	22.3	F	1							Endometriosis, amyloidosis	x			
P346	22.8	F	0			0				Arthritis	x			

Animal	Age (years)	Sex	Histopathology scores of heart and skeletal muscle							Pathologic conditions	Tissues used			
			LV	RV	LA	RA	APE	IVS	RECTF		Heart	Skeltal muscle	Heart ventricle muscle	Dextran Inoc.
L278	24	F	1							Endometriosis	x	x		

LV, left ventricle; RV, right ventricle; LA, left atrium; RA, right atrium; RECTF, *rectus femoris* muscle; APE, apex; IVS, intraventricular septum.

TABLE 2

Antibodies used in this study

Antibodies	Specificity	Clone	Host, Isotype	Dilution	Supplier, Catalogue number
Primary					
Anti-Human Macrophage (Affinity-Purified)	Macrophages, monocytes, capillaries, endothelial cells of smaller blood vessels	HAM56	Mouse, mIgM k	1:50	Affymetrix (Santa Clara, CA, USA), 14654893
CD3	T-cells	n/a	Rabbit, pIgG	1:100	Dako (Agilent Daco, Carpinteria, CA, USA), A0452
CD20cy	B-cells	L26	Mouse, mIgG2a, k	1:200	Dako, M0755
CD163	Pan macrophage marker	10D6	Mouse, mIgG1	1:50	Novocast (Leica Biosystems, Wetzlar, Germany), NCLCD163
CD206	Macrophages, dendritic, endothelial, and epithelial cells	n/a	Rabbit, pIgG	1:50	Sigma (Sigma-Aldrich, St. Louis, MO, USA), HPA004114
Dextran	Amino dextran	DX1	Mouse, mIgG1k	1:50	Stemcell (Stemcell Technologies, Vancouver, British Columbia, Canada), 60026
Dextran	Amino dextran	RA2320SK-PU0299	Chicken, IgY	1:350	Pierce Biotechnology, Inc. (ThermoFisher Scientific Waltham, MA, USA)
Secondary					Thermo Fisher Scientific (Waltham, MA, USA)
Anti-chicken IgY, Alexa 488			Goat, pIgG	1:1000	A11039
Anti-mouse IgM, Alexa 488			Goat, pIgG	1:1000	A21042
Anti-mouse IgG1, Alexa 488/568			Goat, pIgG	1:1000	A21121, A21124
Anti-rabbit IgG, Alexa 488/568			Goat, pIgG	1:1000	A11008, A11011
Anti-rat IgG, Alexa 568			goat, pIgG	1:1000	A11077
Anti-mouse IgG, Alexa 568			goat, pIgG	1:1000	A11031

n/a, not applicable; m, monoclonal; p, polyclonal